A Hybrid Framework for Short-Term Risk Assessment of Wind-Integrated Composite Power Systems

Osama Aslam Ansari, *Student Member, IEEE*, and C. Y. Chung, *Fellow, IEEE*

Abstract— **This paper proposes a new framework for the short-term risk assessment of wind-integrated composite power systems via a combination of an analytical approach and a simulation technique. The proposed hybrid framework first employs the area risk method – an analytical approach, to include the detailed reliability models of different components of a power system. In this regard, a novel reliability modeling approach for wind generation for short-term risk assessment is also proposed. Thereafter, a non-sequential Monte-Carlo simulation (NSMCS) technique is adopted to calculate the partial risks of the area risk method. As a result, the proposed framework is also capable of including the contingencies and constraints of the transmission system that are customarily neglected in the area risk method. The computational performance of the proposed framework is greatly enhanced by adopting the importance sampling (IS) technique whose parameters are obtained using the cross entropy (CE) optimization. Case studies performed on a modified 24-bus IEEE Reliability Test System (RTS) validate that the detailed reliability modeling of wind generation and consideration of the transmission system are necessary to obtain more accurate short-term risk indices. Furthermore, the computational performance of the proposed framework is many orders higher than any other comparable methods.**

Index Terms— **Cross entropy, Monte Carlo simulation, power system operation, reliability modeling, risk assessment.**

I. INTRODUCTION

THE successful transition from the deterministic reliability criterion developed for traditional power systems to the probabilistic methods for modern, renewable-integrated smart grids necessitates the development of both long- and short-term risk assessment methods. Long-term risk assessment methods have been the subject of research for many decades and have been successfully developed and applied in the electric power industry for power systems planning problems [1]–[2]. However, these methods are not applicable to short-term risk assessment during power systems operation owing to two main reasons. First, the long-term risk assessment methods assume the failure probabilities of power systems' components to be independent of time and operating conditions. Second, these techniques do not take into account the decisions taken during the power systems operation, e.g., in unit commitment (UC) and

economic dispatch (ED), while evaluating the risk. Yet, the power systems operators require short-term risk indices to schedule sufficient operating or spinning reserve to account for unplanned contingencies and unexpected variability in generation and load in the coming hours [3].

The PJM method, first proposed in the mid-1960s, is one of the earliest and simplest methods to assess short-term risk for a generating system [3]. The basic PJM method aims to evaluate the probability of a generating system to just meet or fail to meet the expected load during the time in which no additional generation is available. This time is also known as the lead time, and the probability is called the unit commitment risk. Several authors have extended the basic PJM method to consider rapid-start generating units [1], load uncertainty [1]–[2], wind generation [4]–[6], energy storage [7]–[8], and electric vehicles [9] in the evaluation process. Nonetheless, as an essentially analytical approach, the basic PJM method and its variants suffer from two major drawbacks. First, these methods involve state-enumeration techniques whose complexity increases exponentially with the number of power system's component that are included in the evaluation process [2]. Second, analytical methods often incorporate certain simplifications to make the evaluation process tractable. For instance, higher-order contingencies [10] or lower probability events, such as failures of multiple transmission lines in a short time period, are neglected. Because of these reasons, the transmission system's contingencies and constraints might not be incorporated in a straightforward manner. Consequently, the effect of the transmission system on short-term risk might not be conveniently assessed. Ergo, the bus- or load-point short-term risk indices might not be evaluated.

To address the abovementioned limitations, some authors recently proposed simulation-based approaches. In [11], the short-term risk of a composite power system is evaluated using a non-sequential Monte-Carlo simulation (NSMCS). The extremely poor computational performance of Monte-Carlo simulation (MCS) for very low failure probabilities is mitigated by employing an importance sampling (IS) technique. Reference [12] extends the work in [11] to consider renewable generation using quasi-sequential MCS. The variability in the output of renewable generation is modeled using some fixed scenarios, each having same occurrence probabilities. In [13], a state-transition sampling based MCS is employed to compute the short-term risk indices of a composite power system. IS is also utilized to improve the computational speed of the MCS.

In [14], IS is applied to sequential MCS to consider the chronology of failure events in the short-term risk assessment. A bi-level optimization model is proposed in [15] to assess the short-term risk of a transmission system, while neglecting the outages of the generators. In [16], the credibility theory is applied to model the failure probabilities of power systems' components under different weather and operational conditions. Then, the short-term risk is evaluated considering the proposed fuzzy model of failure probabilities. In [17], the computational performance of NSMCS for risk assessment is improved using the subset simulation. Despite the worthy contributions of these works, renewable sources, particularly wind generation, are either not considered at all [11], [13]–[16] or insufficiently modeled [12], [17]. However, the uncertainty introduced by highly variable renewable sources coupled with the limitations of the transmission system can have a measurable impact on the short-term risk of composite power systems.

Analytical approaches can allow for detailed reliability modeling of wind generation in short-term risk assessment [4], [5], whereas simulation techniques are robust and can consider the transmission system as well as different operational characteristics of a power system [11], [14]. The purpose of this paper is therefore to propose a hybrid framework that makes use of the aforesaid advantages of analytical and simulation techniques to duly evaluate the short-term risk of a wind-integrated composite power system.

To suitably assess the impact of wind generation on short-term risk, a novel reliability modeling approach for wind generation is first proposed. The proposed modeling approach employs conditional probability distributions of wind speed, conditional probabilities, and the law of total probability to effectively model the probable variations in the output of wind generation during the lead time. The area risk method, which is an extension of the basic PJM method, is then modified and extended to include the proposed reliability modeling approach.

Thereafter, the modified area risk method is innovatively amalgamated with the NSMCS to calculate the partial risks of the area risk method. The requirements for computational memory and reliability data for the NSMCS are lower than other MCS techniques. To improve the computational performance of the proposed framework, the IS technique is applied to the NSMCS. In addition to the generators and transmission lines, the IS technique is directly applied to the wind speed distributions for wind generation. The parameters of the IS technique are obtained using iterative cross entropy (CE) optimization, which is one of the most widely adopted methods to obtain the near-optimal IS parameters [18], [19].

The proposed framework is applied to a modified IEEE Reliability Test System (RTS) to indicate its effectiveness in efficiently computing the short-term risk indices of a wind-integrated composite power system. The short-term risk indices are also evaluated for the commitment schedules obtained from the day-ahead UC (DAUC) program to show its application in power systems operation.

The main contributions of this work are as follows:
1. A novel hybrid framework for short-term risk assessment is proposed. The framework exploits the advantages of the area risk method and NSMCS to suitably assess the short-term risk of wind-integrated composite power systems. The proposed framework can also evaluate the bus- or load-point indices.
2. To obtain accurate short-term risk indices, a new reliability modeling approach for wind generation is also proposed. This approach effectively models the uncertainty of wind generation in the operational domain through conditional distributions. Additionally, the area risk method is modified to include the proposed reliability modeling approach.
3. The computational speed of the proposed hybrid framework is greatly enhanced by adopting the CE-based IS technique for NSMCS. The IS technique is also applied to the conditional distributions of wind speed.

The rest of the paper is organized as follows. Section II provides a preliminary description of the area risk method. Section III delineates the proposed reliability modeling approach for wind generation. The proposed hybrid framework is explained in Section IV. Case studies are performed in Section V. Finally, Section VI concludes the paper.

II. PRELIMINARIES OF THE AREA RISK METHOD

The area risk method, which is an extension of the basic PJM method, was first proposed to consider rapid start generating units in the evaluation of short-term risk [1]. The area risk method divides the given lead time into several sub-periods, and the partial risk in each sub-period is obtained using the basic PJM method. The summation of these partial risks gives the overall short-term risk for a given lead time. Consequently, the area risk method can consider the varying operational states of a power system within a lead time. As an example, Fig. 1 pictorially depicts the area risk method for a given lead time that is divided into three sub-periods. Note that this representation only portrays the area risk method and does not necessarily represent the actual short-term risk indices.

After dividing the lead time into appropriate sub-periods, the next step is to obtain suitable reliability models of different components of a power system for each sub-period of the area risk method.

A. Conventional Generators Modeling

Reliability modeling of conventional generators for short-term risk assessment is based on the assumption that the lead time is sufficiently short to ignore any repair processes [1]. Therefore, the probability of a generating unit on outage, also known as the outage replacement rate (ORR), is given by the following exponential distribution:

$$ORR_g = 1 - e^{-\lambda_g t} \approx \lambda_g t, \quad \forall g \in \{1, \dots, N^G\}, \quad (1a)$$

where each generating station g consists of N^g identical generating units with ORR_g, λ_g is the failure rate in failures per hour of a generating unit in generating station g, t is the lead time, and N^G is the total number of generating stations in the power system. Note that because of its memoryless property, the exponential distribution inherently models the dependence of a random variable (in this case, time to fail t) between the

sub-periods [20]. In other words, the failure time of a generating unit in a certain sub-period is dependent on the generating unit's outage history in the previous sub-periods.
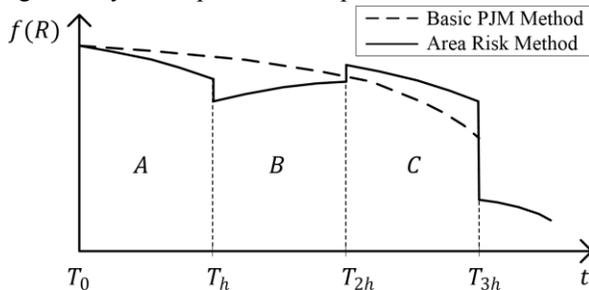
Fig. 1. Pictorial representation of the area risk method. T_0 represents the initial hour. T_h, T_{2h}, and T_{3h} represent one, two, and three hour(s), respectively, after the initial hour.

B. Transmission Lines Modeling

In the original area risk method and its variants [4]–[9], the transmission system is generally ignored. However, transmission line outages coupled with line flow limits might also result in load curtailment, which contributes to the short-term risk. Therefore, in this work, the transmission system is taken into account for accurate short-term risk evaluation. The inclusion of transmission system also allows for the calculation of bus-point indices. Similar to the modeling of conventional generators, the repair process is ignored and the exponential distribution is assumed. Consequently, the transmission lines are also modeled using ORR. For a line l:

$$ORR_l = 1 - e^{-\lambda_l t} \approx \lambda_l t, \quad \forall l \in \{1, \dots, N^L\}, \quad (1b)$$

where λ_l is the failure rate in failures per hour of transmission line l and N^L is the total number of transmission lines.

III. PROPOSED RELIABILITY MODELING OF WIND GENERATION

Aptly modeling the variability of wind generation during the lead time is vital to precisely assess the short-term risk of a wind-integrated power system. The wind generation fluctuates with the wind speed that is highly irregular and variable. Hence, a single ORR, as used for conventional generators, cannot represent the wind generation's capacity outages in short-term risk assessment methods.

One approach to modeling the wind generation is through the probabilistic modeling of wind speed during the lead time. The wind speed in a short future time period strongly depends on the initial wind speed at the start of that time period. This observation has been adopted in [4] and [5]. In particular, [4] obtains the conditional probability density functions (PDFs) of wind speed for different sub-periods in the lead time for a given initial wind speed at the start of the lead time (T_0 in Fig. 1). The initial wind speed at T_0 is deterministically known, along with other operational statuses during power systems operation. The conditional PDFs are then converted to wind power PDFs using the wind turbine's power curve. Fig. 2 represents these conditional PDFs of wind speed for a given initial wind speed at T_0 in different sub-periods for an actual wind farm site. In this approach, the initial wind speeds at the start of subsequent sub-periods (i.e., at T_h and T_{2h}) are ignored.
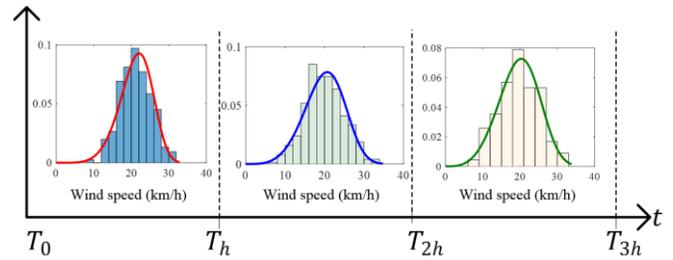
Fig. 2. Conditional PDFs of wind speed in different sub-periods for a single initial wind speed at T_0.
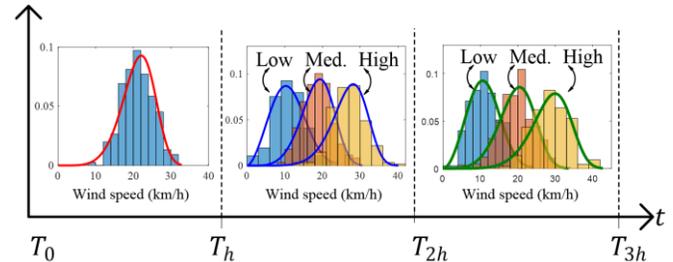
Fig. 3. Conditional PDFs of wind speed in different sub-periods for different initial wind speeds at the start of those sub-periods.

Due to the highly volatile nature of wind speed, considering only a single wind speed PDF during each sub-period might not truly capture its spasmodic variations. Also, the wind speed PDFs during different sub-periods can be poles apart depending on the initial wind speeds at the start of the respective sub-periods. In other words, the wind speed PDFs during different sub-periods should be conditional on the initial wind speed at the start of the respective sub-periods, and not at the start of the lead time. Fig. 3 illustrates the abovementioned statements. For the second sub-period B (T_h- T_{2h}), the conditional PDFs of wind speed for three arbitrarily chosen initial wind speeds (low, 10 km/h; medium, 20 km/h; high, 30 km/h) at the start of the second sub-period (T_h) are shown. A comparison with Fig. 2 shows that the conditional PDFs of wind speed in the second sub-period are markedly different from the one obtained by assuming a single initial wind speed at the start of the entire lead time. Similar conclusions can be drawn about the conditional PDFs of wind speed in the third sub-period C (T_{2h}-T_{3h}). Hence, the conditional PDFs of wind speed in a sub-period must consider the probable initial wind speeds at the start of that sub-period. These probable initial wind speeds at the start of a sub-period, in turn, depend on the conditional PDF in the preceding sub-period.

To understand the impact of different modeling approaches of PDFs on the risk assessment, first, the risk is generally defined as follows [18]:

$$Risk = \int H(x)F(x)dx, \quad (2a)$$

where, $H(\cdot)$ is a test function and will be explained later. $F(\cdot)$ is the joint PDF of a random vector X. For composite power systems,

$$F(X) = f^G(X^G)f^L(X^L)f_P^{ws}(X^w), \quad (2b)$$

where, $f^G(X^G)$ is the PDF for random vector X^G, which represents the number of available generating units in each generating station, $f^L(X^L)$ is the PDF for random vector X^L representing the availability of transmission lines, and $f_P^{ws}(X^w)$ is the PDF for random vector of wind speed X^w in a period P. Note that $X = [X^G, X^L, X^w]$. $f^G(X^G)$ and $f^L(X^L)$ can be

calculated using (1a) and (1b), respectively. From (2a) and (2b), it is clear that the choice of PDFs directly affects the risk indices. Hence, a more precise determination of $f_P^{ws}(X^w)$ will expectedly result in more accurate risk indices.

Now using the above notation, according to [4],

$$f_B^{ws}(v^B) = f_{B|A}^{ws}(v^B|v^A), \quad f_C^{ws}(v^B) = f_{C|B}^{ws}(v^B|v^C), \quad (2c)$$

where, $f_{B|A}^{ws}(v^B|v^A)$ is the conditional PDF for sub-period B given a PDF for sub-period A, and $f_{C|B}^{ws}(v^B|v^C)$ is the conditional PDF for sub-period C given a PDF for sub-period B. In other words, (2c) implies that the PDFs for sub-periods B and C are assumed to be independent of the PDFs for sub-periods A and B, respectively. This independence assumption indicates the lack of information about the model.

As shown in Fig. 3 and its corresponding discussion, a more reasonable approach is to model the PDFs for sub-periods B and C, considering their dependence on the PDFs for sub-periods A, and B, respectively. By the law of total probability, these PDFs can be obtained as

$$f_B^{ws}(v^B) = \int_{-\infty}^{\infty} f_{B|A}^{ws}(v^B|v^A) f_A^{ws}(v^A) dv^A, \quad (2d)$$

$$f_C^{ws}(v^C) = \int_{-\infty}^{\infty} f_{C|B}^{ws}(v^C|v^B) f_B^{ws}(v^B) dv^B. \quad (2e)$$

In this work, a systematic approach based on probabilistic techniques, is proposed to consider (2d) and (2e) for the short-term risk assessment. In what ensues, the proposed approach is explained by considering a lead time of 3 hours as an example. For a specific power system, the actual determination of a suitable lead time depends on the start-up times of rapid-start generating units [3]. Also, as an example, the lead time is divided into three hourly sub-periods. Note that the choice of hourly sub-periods is motivated by the typical one-hour intervals considered in the UC programs. However, the systematic approach presented here is generally applicable to any length of lead time and for any number of sub-periods.

Referring to Fig. 1, as a first step, using the known initial wind speed ($v^{ini,A}$) at the start of the lead time, i.e. at the start of sub-period A, the conditional PDF of wind speed for sub-period A, $f_A^{ws}(v^A)$, is obtained using Algorithm 1. In Algorithm 1, for $f_A^{ws}(v^A)$, the given hour is T_0 and the hth hour is T_h.

Algorithm 1 Algorithm for Wind Speed Conditional PDFs

Input: Mean and standard deviation of historical hourly wind speeds, autoregressive moving average (ARMA) series of wind speed, and initial wind speed of a given hour

Output: Conditional Weibull PDF of wind speed for the next hth hour

1: Simulate the ARMA series of wind speed using historical hourly wind speed data for a large number of simulation years N ($\sim 5000 - 10,000$ years) [5], let Λ be the set of simulated wind speed values, then $\Lambda = \{v_s^{t,\eta}\}, t \in \{1, \dots, 8760\}, \eta \in \{1, \dots, N\}$, where $v_s^{t,\eta}$ is the simulated wind speed in hour t and year η.

2: Define an interval Δv (e.g., 1 km/h) around the initial wind speed of the given hour

3: Group all those simulated wind speed values of the next hth hour, provided that the simulated wind speed values of the given hour lie in the interval around the initial wind speed, i.e. $\Psi = \left\{ v_s^{T_0+h,\eta} : v_0^{T_0} - \frac{\Delta v}{2} \le v_s^{T_0,\eta} \le \right.$

$\left. v_0^{T_0} + \frac{\Delta v}{2} \right\}, \eta \in \{1, \dots, N\}$, where $\Psi \subset \Lambda$ is the set of grouped simulated wind speed values $v_s^{T_0+h}$ of hth hour, $v_s^{T_0}$ is the simulated wind speed values of given hour, $v_0^{T_0}$ is the initial wind speed at given hour T_0

4: Fit a Weibull PDF to the set Ψ, i.e., $f_h^{ws}(\cdot) = $ Weib(a, b), where a is the scale parameter and b is the shape parameter.

Next, the PDF for the first sub-period A is divided into N^p partitions. The midpoints of these partitions are assumed to be estimates of initial wind speeds for the start of sub-period B i.e., at T_h. These midpoints are obtained using (3a)–(3c):

$$p_i^A = \underline{v^A} + i\left(\overline{v^A} - \underline{v^A}\right)/N^p, \quad \forall i \in \{1, \dots, N^p - 1\}, (3a)$$

$$v_j^{ini,B} = (p_{j-1}^A + p_j^A)/2, \quad \forall j \in \{2, \dots, N^p - 1\}, \quad (3b)$$

$$v_1^{ini,B} = (\underline{v^A} + p_1^A)/2, \quad v_{N^p}^{ini,B} = (p_{N^p-1}^A + \overline{v^A})/2, \quad (3c)$$

where p_i^A and $v_j^{ini,B}$ are the partitioning points of $f_A^{ws}(v^A)$ and the estimated initial wind speeds, respectively. $\overline{v^A}$ and $\underline{v^A}$ are the maximum and minimum observed wind speed values of v^A in sub-period A, respectively.

Each of these estimated initial wind speeds have associated occurrence probabilities that can be calculated using (3d)–(3f):

$$P(v_j^{ini,B}) = \int_{p_{j-1}^A}^{p_j^A} f_A^{ws}(v^A) dv^A, \forall j \in \{2, \dots, N^p - 1\} (3d)$$

$$P(v_1^{ini,B}) = \int_0^{p_1^A} f_A^{ws}(v^A) dv^A, \quad (3e)$$

$$P(v_{N^p}^{ini,B}) = \int_{p_{N^p-1}^A}^{\infty} f_A^{ws}(v^A) dv^A, \quad (3f)$$

where $P(v_j^{ini,B})$ is the probability of initial wind speed $v_j^{ini,B}$. Note that $\sum_{j=1}^{N^p} P(v_j^{ini,B}) = 1$.

Fig. 4 depicts these estimated initial wind speeds using the conditional PDF of wind speed for sub-period A with $N^p = 3$. For this case, these three initial wind speeds might correspond to low, medium and high initial wind speed scenarios, having corresponding occurrence probabilities as illustrated by the shaded region in the figure.

Now, for each of these estimated initial wind speeds, conditional PDFs of wind speed for sub-period B are obtained using Algorithm 1. In this case, the initial hour is set to the start of sub-period B (T_h) and the hth hour is set to the end of sub-period B (T_{2h}). As a result, a total of N^p conditional PDFs ($\{f_{B,1}^{ws}, \dots, f_{B,N^p}^{ws}\}$) are obtained that represent the variability of wind speed for this sub-period. This statement can be interpreted as follows. As the uncertainty of wind speed increases with future time, multiple PDFs are employed to represent this increased uncertainty. Moreover, each of these conditional PDFs also have occurrence probabilities given by (3d)–(3f).

By following a similar approach, the estimates of initial wind speed at the start of sub-period C ($v_j^{ini,C}$) can be obtained by further dividing each of the N^p conditional PDFs of sub-period B into N^p partitions. However, this division would result in $N^p \times N^p$ estimates of initial wind speed and conditional PDFs for sub-period C, thereby requiring $N^p \times N^p$ computations of partial risks. To circumvent the problem of high computational burden and intractability, first a surrogate conditional PDF of

wind speed for sub-period B is estimated using the initial wind speed at the start of sub-period A via Algorithm 1. Afterward, this surrogate conditional PDF is divided into N^{p} partitions resulting in N^{p} estimated initial wind speeds for the start of sub-period C. Then, the conditional PDFs of wind speed for sub-period C ($\{f_{C,1}^{ws}, \dots, f_{C,N^{\mathrm{p}}}^{ws}\}$) are obtained using these estimated initial wind speed values via Algorithm 1. As a result, the conditional PDFs for sub-period C are still dependent on the initial wind speeds at the start of sub-period C, while the number of conditional PDFs remains N^{p}. The whole process can be repeated for any number of sub-periods of the area risk method and for any $N^{\mathrm{p}} > 1$.
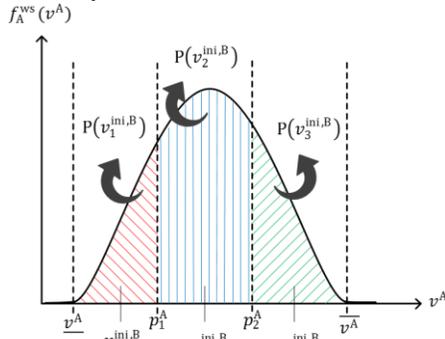
Fig. 4. Partitioning of the conditional PDF of wind speed.

IV. PROPOSED RISK ASSESSMENT FRAMEWORK

In this section, the proposed framework for the short-term risk assessment of wind-integrated composite power systems is explained. The key ingredients of the proposed framework are the modified area risk method considering the proposed reliability modeling of wind generation and the IS-based NSMCS. The short-term risk index considered in this paper is the probability index, i.e., the probability of load curtailment. Nonetheless, the framework can be easily extended to evaluate other risk indices, such as expected power not supplied and expected number of load curtailments.

A. Modified Area Risk Method

The area risk method needs to be adapted to consider the proposed reliability modeling of wind generation. Note that, for each sub-period B and C, N^{p} partial risks, corresponding to N^{p} conditional PDFs of wind speeds, must be evaluated. Also, because each of these N^{p} partial risks represent disjoint events, the law of total probability can be applied to obtain the net partial risks. For sub-periods B and C, the net partial risks are given by (4a)–(4b), and the total risk is then evaluated by (4c):

$$R_B = \sum_{j=1}^{N^{\mathrm{p}}} \mathrm{P}\left(v_j^{\mathrm{ini,B}}\right) \cdot PR_j^B - R_A, \tag{4a}$$

$$R_C = \sum_{j=1}^{N^{\mathrm{p}}} \mathrm{P}\left(v_j^{\mathrm{ini,C}}\right) \cdot PR_j^C - R_B, \tag{4b}$$

$$R = R_A + R_B + R_C, \tag{4c}$$

where PR_j^B is the partial risk in sub-period B considering the jth conditional PDF of wind speed v^B. Similarly, PR_j^C represents the partial risk in sub-period C considering the jth conditional PDF of wind speed v^C. R_A, R_B, and R_C are the net partial risks for sub-periods A, B, and C, respectively. R is the total risk for the entire lead time. Equations (4a) and (4b) can be viewed as discrete approximations to (2d) and (2e),

respectively. Fig. 5 pictorially represents the modification to the area risk method for $N^{\mathrm{p}} = 3$.
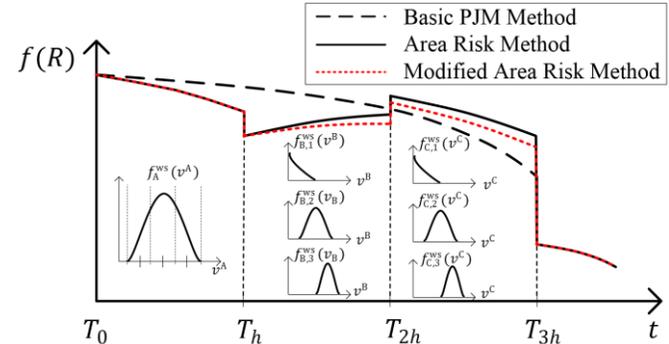
Fig. 5. Integrating the proposed reliability modeling of wind generation in the area risk method.

B. Evaluation of Partial Risks via CE-MCS

The routinely employed approach to evaluate the partial risks in the area risk method is to use a capacity outage probability table (COPT), which is, in essence, an analytical method. As mentioned in the Introduction, analytical methods are not appropriate for composite power system risk assessment. Therefore, a more prudent approach is to employ a simulation technique such as NSMCS. Simulation techniques are robust to system size and can also consider a wide range of operational characteristics. Therefore, this work proposes a fusion of the area risk method with NSMCS to adequately assess the short-term risk of a composite power system.

Using crude NSMCS, the jth partial risk for any sub-period P can be evaluated as

$$PR_j^P = \frac{1}{N^{\mathrm{sim}}} \sum_{k=1}^{N^{\mathrm{sim}}} H(\boldsymbol{X}_k; L), \tag{5a}$$

where $\boldsymbol{X}_k = [\boldsymbol{X}_k^G, \boldsymbol{X}_k^L, \boldsymbol{X}_k^W]$, $\boldsymbol{X}_k^G = [n_k^1, \dots, n_k^g, \dots, n_k^{N^G}]$, $\boldsymbol{X}_k^L = [\zeta_k^1, \dots, \zeta_k^l, \dots, \zeta_k^{N^L}]$, and $\boldsymbol{X}_k^W = [v_k^1, \dots, v_k^w, \dots, v_k^{N^W}]$. $\boldsymbol{X}_k^G$ and $\boldsymbol{X}_k^L$, are the kth samples following $\mathrm{B}(\boldsymbol{X}; \boldsymbol{N}^g, \boldsymbol{ORR}_G)$ and $\mathrm{B}(\boldsymbol{X}; \boldsymbol{1}, \boldsymbol{ORR}_L)$, respectively, where $\mathrm{B}(\cdot; \cdot, \cdot)$ stands for the binomial distribution [18]. $\boldsymbol{ORR}_G$ and $\boldsymbol{ORR}_L$ are vectors of ORRs for the generating stations and transmission lines, respectively. n_k^g represents the number of available generating units in generating station g having a total of N^g generating units. $\boldsymbol{N}^g$ is a vector of the number of generating units N^g. ζ_k^l is 1 if line l is available and 0 if it is on outage. v_k^w is the kth wind speed sample following the jth conditional PDF of the wind speed of wind farm w, $f_{P,j}^{ws,w}(\boldsymbol{X}_k^W)$. N^W is the number of wind farms. N^{sim} is the number of samples. Note that R_A in (4c) can also be calculated using (5a).

In (5a), $H(\boldsymbol{X}_k; L)$ is a test function that evaluates whether or not the sample $\boldsymbol{X}_k$ leads to load curtailment. For the short-term risk assessment of a generating system,

$$H(\boldsymbol{X}_k; L) = \begin{cases} 0 & S(\boldsymbol{X}_k) \geq L \\ 1 & S(\boldsymbol{X}_k) < L \end{cases}, \tag{5b}$$

where $S(\boldsymbol{X}_k)$ represents the summation of available generation capacity associated with state $\boldsymbol{X}_k$, and L is the load. For composite power systems, the definition of $S(\boldsymbol{X}_k)$ is modified, as the transmission system should also be considered to determine the load curtailment. In this regard, the DC representation of transmission system is adopted in this work.

The DC optimal power flow (DC-OPF) is employed to evaluate the load curtailment at each bus for each state X_k. If no load curtailment occurs at any bus, $S(X_k)$ is the same as that obtained for the generating system. However, if the load curtailment is non-zero, $S(X_k)$ is given by:

$$S(X_k) = \sum_{b=1}^{N^B} l_b, \tag{5c}$$

where l_b is the load served at bus b and N^B is the total number of buses in the system. l_b is obtained using the DC-OPF.

A fundamental downside of the crude NSMCS is the large computational burden when the events to be assessed are rare i.e. for *rare event simulation* [18]. This is the case in the short-term risk assessment as the probability of load curtailment in a short lead time is often very small (around ~10^{-4}). Also, because N^P partial risks are required to be evaluated for each of sub-periods B and C, the direct application of the crude NSMCS is computationally prohibitive. Hence, in this work, the IS technique is applied to improve the computational performance of the crude NSMCS. The IS is a variance reduction technique in which the original probability distributions are distorted to increase the occurrences of failure events, thereby accelerating the convergence rate of simulation. In this case, IS modifies $B(\cdot; N^g, ORR_G)$ and $B(\cdot; 1, ORR_L)$ to $B(\cdot; N^g, ORR_G^*)$ and $B(\cdot; 1, ORR_L^*)$, respectively. In addition, in this work, the original conditional PDF of the wind speed is distorted from $f_{P,j}^{ws,w}(\cdot)$ to $f_{P,j}^{ws,w,*}(\cdot)$. $f_{P,j}^{ws,w}(\cdot)$ is a Weibull distribution with two parameters (a_w, b_w); however, only the scale parameter (a_w) is modified. These distorted PDFs, also known as the IS densities, are then used to obtain the new samples X_k. The partial risk is then evaluated by the following unbiased estimator:

$$PR_j^P = \frac{1}{N^{sim}} \sum_{k=1}^{N^{sim}} H(X_k; L) W(X_k), \tag{5d}$$

where $W(X_k)$ is the likelihood ratio and given by:

$$W(X_k) = W_G(X_k) W_L(X_k) W_W(X_k), \tag{5e}$$

$$W_G(X_k) = B(X_k^G; N^g, ORR_G) / B(X_k^G; N^g, ORR_G^*), \tag{5f}$$

$$W_L(X_k) = B(X_k^L; 1, ORR_L) / B(X_k^L; 1, ORR_L^*), \tag{5g}$$

$$W_W(X_k) = \prod_{w=1}^{N^W} \left(f_{P,j}^{ws,w}(X_k^W) / f_{P,j}^{ws,w,*}(X_k^W) \right). \tag{5h}$$

Different methods can be employed to obtain the IS densities [18], [19]. The most widely used approach is the CE optimization, which minimizes the Kullback-Leibler divergence between the optimal IS densities and the approximated IS densities. In this work, the CE optimization is adopted to find the IS densities for generators, transmission lines, and wind speed. Interested readers are referred to [19] for a detailed discussion on the CE optimization and to [21]–[23] for its initial application to the long-term risk assessment of power systems. For the sake of simplicity, the CE optimization is presented here as Algorithm 2, without detailing each step.

The combination of the CE optimization with NSMCS will be referred to, henceforward, as the CE-MCS.

Algorithm 2 CE Optimization

Input: Original ORRs of generating units and transmission lines, Weibull PDF of wind speed and load L

Output: Distorted ORR of generating units and transmission lines, and distorted Weibull PDF of wind speed

1:      Set the number of samples for CE optimization (N^{CE}), and other CE parameters (ρ, α, m^{max})

2:      Obtain the original vectors of ORRs and $f_{P,j}^{ws,w}(\cdot)$

3:      Set iteration counter $m = 1$, $ORR_G^m = ORR_G$, $ORR_L^m = ORR_L$, and $f_{P,j}^{ws,w,m}(\cdot) = f_{P,j}^{ws,w}(\cdot)$

4:      **for** $m = 1$ to $m = m^{max}$ **do**

5:      Obtain samples $X_p = [X_p^G, X_p^L, X_p^W]$, where $p = \{1, ..., N^{CE}\}$, following $B(\cdot; N^g, ORR_G^m)$, $B(\cdot; N^g, ORR_L^m)$, and $f_{P,j}^{ws,w,m}(\cdot)$

6:      Evaluate the performance function $S(X_p)$ and arrange $S(X_p)$ in ascending order, i.e., $S[1] \leq S[2] \leq \cdots \leq S[N^{CE}]$

7:      **if** $(S[\lfloor \rho N^{CE} \rfloor] \geq L)$, set $\widehat{L_m} = S[\lfloor \rho N^{CE} \rfloor]$ **else** set $\widehat{L_m} = L$

8:      Evaluate the test function $H(X_p; \widehat{L_m})$ for all p

9:      Calculate $W_G(X_p), W_L(X_p)$, and $W_W(X_p)$ using (5f)–(5h), also calculate $W(X_p)$ using (5e), for all p

10:      Calculate the distorted ORRs and scale parameter:

$$ORR_g^{m+1} = \alpha \left(1 - \frac{1}{N^g} \frac{\sum_{p=1}^{N^{CE}} H(X_p; \widehat{L_m}) W(X_p) n_p^g}{\sum_{p=1}^{N^{CE}} H(X_p; \widehat{L_m}) W(X_p)} \right) + (1 - \alpha) ORR_g^m$$

$$ORR_l^{m+1} = \alpha \left(1 - \frac{\sum_{p=1}^{N^{CE}} H(X_p; \widehat{L_m}) W(X_p) \zeta_p^l}{\sum_{p=1}^{N^{CE}} H(X_p; \widehat{L_m}) W(X_p)} \right) + (1 - \alpha) ORR_l^m$$

$$a_w^{m+1} = \left(\frac{\sum_{p=1}^{N^{CE}} H(X_p; \widehat{L_m}) W(X_p) (v_p^w)^{b_w}}{\sum_{p=1}^{N^{CE}} H(X_p; \widehat{L_m}) W(X_p)} \right)^{1/b_w}$$

11:      **if** $\widehat{L_m} = L$, break the **for** loop

12:      Set $ORR_G^* = ORR_G^m$, $ORR_L^* = ORR_L^m$, and $f_{P,j}^{ws,w,*}(\cdot) = f_{P,j}^{ws,w,m}(\cdot)$

C. Overall Framework

The complete hybrid framework for the short-term risk assessment of wind-integrated composite power systems is given in Fig. 6. The first step of the framework involves determining the committed generating units through a UC program. Then, the modified area risk method is utilized and the partial risk for the first sub-period is obtained using the CE-MCS presented in Section IV-B. Thereafter, N^P partial risks are evaluated using (5d) for each subsequent sub-period. Finally, the total risk is evaluated using (4c). Note that the parallel computational techniques can be applied to calculate the partial risks for all sub-periods at the same time. To this end, the framework in Fig. 6 can be slightly modified. The step for calculating the net partial risks ((4a) and (4b)) after evaluating partial risks for all conditional PDFs for a sub-period can be deferred, and the partial risks for all sub-periods can be calculated first. This allows steps in the larger grey rectangles in Fig. 6 to be run on separate cores of a PC at the same time.

With regard to the evaluation of bus-point indices, the only modification required to the proposed framework is a change in the definition of test function $H(X_k; L)$. In this case, $H(X_k; L)$ must be defined for each bus in the power system as follows:

$$H_b(X_k; L_b) = \begin{cases} 0 & l_b \geq L_b \\ 1 & l_b < L_b \end{cases}, \tag{6a}$$

where $H_b(\boldsymbol{X}_k; L_b)$ is the test function for bus b, L_b is the load demand at bus b. After defining the test function, the rest of procedure is similar, and the partial risk is calculated using:

$$PR_{j,b}^{\mathrm{P}} = \frac{1}{N^{\mathrm{sim}}} \sum_{k=1}^{N^{\mathrm{sim}}} H_b(\boldsymbol{X}_k; L_b) \, W(\boldsymbol{X}_k), \qquad (6b)$$

where $PR_{j,b}^{\mathrm{P}}$ is the partial risk for bus b in sub-period P considering the jth conditional PDF of wind speed.
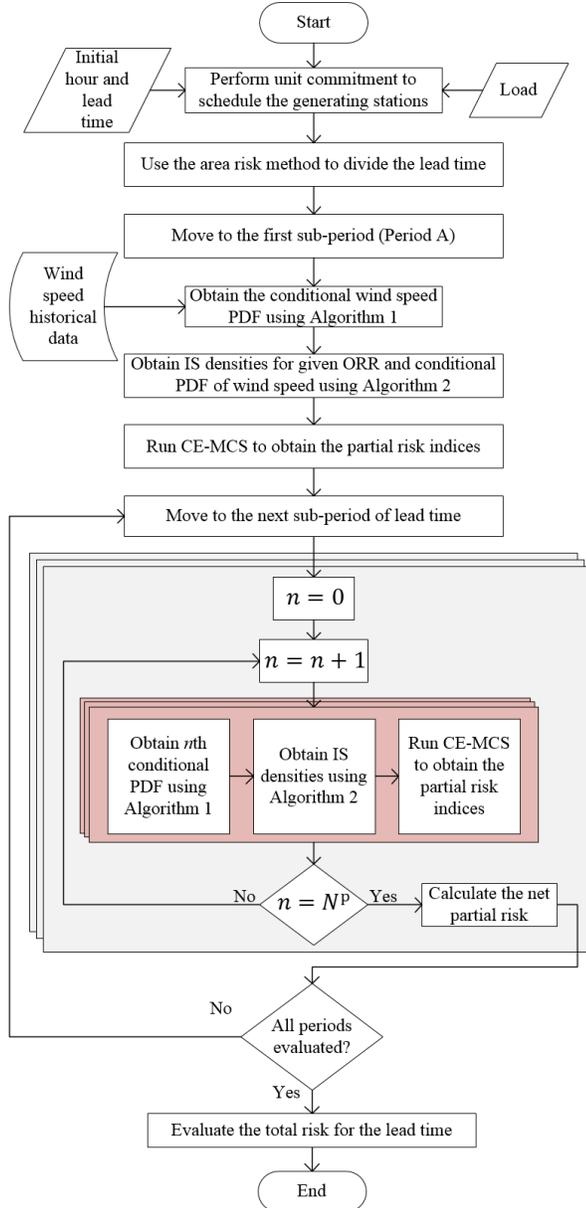
Fig. 6. Proposed hybrid framework for the short-term risk assessment.

V. CASE STUDIES

In this section, the effectiveness of the proposed framework is demonstrated through some key simulations performed on the modified 24-bus IEEE RTS [24]. The original RTS comprises 14 generating stations with 32 generating units in total, 24 buses, 17 load points, and 33 transmission lines. The original RTS is modified by including a 1,000 MW wind farm at bus 14. Also, a 155 MW conventional generator at bus 16 is removed. For CE optimization, N^{CE} is set between 20,000 and 50,000, ρ is set between 0.01 and 0.05, α is set to 0.95, and

m^{max} is set to 10. These parameters are obtained from [19] and [21]. For the convergence of MCS, the minimum coefficient of variation (COV) is set to 2% for the generating system and 5% for the composite power system. In all simulations, the lead time is equal to 3 hours and N^{P} is set to 3. The ARMA series for Algorithm 1, along with the wind turbine curve, is obtained from [25]. All studies are performed for January 31 from hours 00:00 to 04:00, unless otherwise stated. Note that these specific hours are only selected for case studies. As it will be shown later, the proposed framework is generally applicable for any time of the day. All simulations are performed on a PC with a 3.40 GHz Intel® Core i7-4770 CPU and 16 GB RAM. The proposed framework is implemented in MATLAB R2015a, with GUROBI 7.0.2 used as a solver for DC-OPF.

A. Demonstrative Case

To confirm the efficacy of the proposed reliability modeling approach of wind generation, the proposed framework is compared with the approaches presented in [4] and [5]. Because [4] and [5] do not consider the transmission system, it is ignored in this subsection for the sake of comparison. The load is set to the peak value of 2,850 MW, and all 31 generating units are committed to supply the load.

Table I presents the short-term risk indices for different initial wind speeds at the start of the lead time. The short-term risk indices obtained from the proposed framework lie between the ones estimated by [4] and [5]. In other words, [4] ([5]) may overestimate (underestimate) the short-term risk indices. The aforementioned observation holds for all initial wind speed values. One reason for this behavior can be elucidated with the help of Table II, which depicts the mean wind speeds and corresponding occurrence probabilities for each sub-period in all three approaches when the initial wind speed is 20 km/h. For example, for sub-period B, [4] assumes a mean wind speed of 19.94 km/h with a probability of 100%. However, there is actually a 26.39% chance that the mean wind speed during sub-period B is 25.63 km/h. Higher mean wind speeds correspond to higher wind generation and, therefore, lower risk indices. On the other hand, [5] assumes a mean wind speed of 19.71 km/h for the entire lead time and thus neglects any possible low wind speed values that might occur within different sub-periods of the lead time. Hence, the risk obtained by [5] is lower. By considering the multiple conditional PDFs during sub-periods B and C, the proposed approach accounts for the probable variations in the wind speed and, consequently, in wind generation during these sub-periods, thereby resulting in more realistic risk evaluation.

To further investigate the accuracy of the proposed reliability modeling approach, the regression analyses between wind generation values of different sub-periods are exhibited in Fig. 7. A close scrutiny of Fig. 7 reveals two important insights. Firstly, the linear regression models in sub-periods B and C are evidently different when the initial wind power (or initial wind speed) at the start of the respective sub-periods (i.e., at T_h, and T_{2h}, respectively) are considered. This observation reinforces the point made in Section II that the wind speed PDFs of sub-periods should be conditional on the initial wind speeds at the start of respective sub-periods. Secondly, compared to Fig. 7(a) and Fig. 7(b), the linear regression models in Fig. 7(c)

This article has been accepted for publication in a future issue of this journal, but has not been fully edited. Content may change prior to final publication. Citation information: DOI 10.1109/TPWRS.2018.2881250, IEEE Transactions on Power Systems

8

and Fig. 7(d), respectively, indicate higher wind generation in those sub-periods. The higher wind generation will expectedly result in lower probabilities of load curtailment. As a result, the short-term risk indices obtained using the proposed approach are lower than those calculated from [4] in Table I.

TABLE I
SHORT-TERM RISK FOR DIFFERENT WIND GENERATION MODELING METHODS

Initial Wind Speed	Case	R_A (× 10^{-4})	R_B (× 10^{-4})	R_C (× 10^{-4})	R (× 10^{-4})
10 km/h	Proposed	0.5011	1.3768	2.7686	4.6465
	[4]	0.5011	1.9990	4.2676	6.7677
	[5]	-			4.2690
20 km/h	Proposed	0.2630	0.9939	1.7637	3.0206
	[4]	0.2630	1.2337	2.8485	4.3452
	[5]	-			2.7855
30 km/h	Proposed	0.0384	0.2735	1.1404	1.4523
	[4]	0.0384	0.2782	1.2073	1.5239
	[5]	-			1.2634

TABLE II
MEAN WIND SPEED DURING DIFFERENT SUB-PERIODS

Case	Period A (km/h)	Period B (km/h)	Period C (km/h)
Proposed	21.15 (1) †	12.05 (0.1290)	12.43 (0.2434)
		18.72 (0.6071)	20.55 (0.6058)
		25.63 (0.2639)	27.93 (0.1508)
[4]	21.15 (1)	19.94 (1)	19.71 (1)
[5]		19.71 (1)	

†The numbers in brackets indicate the corresponding occurrence probabilities.
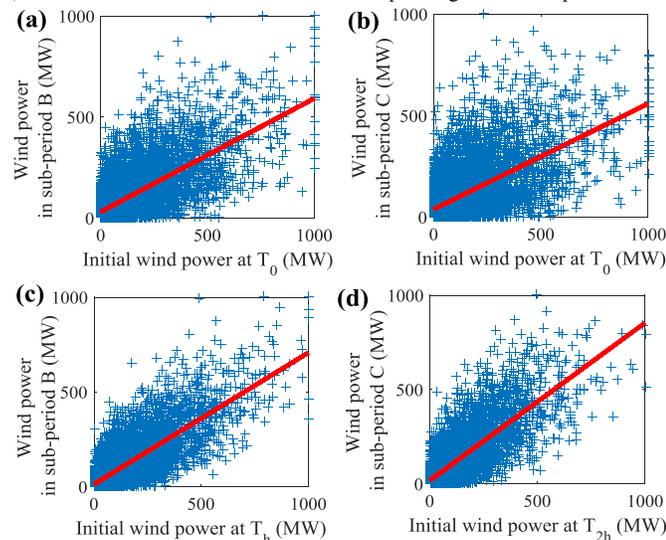
Fig. 7. Regression analyses, (a), (b): using the approach of [4], and (c), (d): using the proposed approach.

B. Computational Performance

From the power system operators' perspective, the computational speed of short-term risk assessment framework is of great importance in order to make timely risk-informed decisions. Ergo, in this subsection, the computational speed of the proposed framework is examined. For a COV of 2%, crude NSMCS would require nearly ~10^8 samples to evaluate the risk which is on the order of ~10^{-4} [18]. This means one complete risk evaluation for the entire lead time would require approximately ~7×10^8 samples. This, in turn, would result in extremely large computational times. Therefore, to compare the computational performances of the CE-MCS with the crude NSMCS within a suitable simulation time, the system is made less reliable by removing a 155 MW conventional generator at

bus 15 and assessing the short-term risk indices of the resulting generating system. For this modified system, Table III compares the computational performances of the crude NSMCS against the CE-MCS, while considering the initial wind speed of 20 km/h. The computational performance of the CE-MCS is several orders higher than that of the crude NSMCS. The poor performance of the crude NSMCS is due to very low failure probabilities of the power system components during a short lead time.

TABLE III
COMPUTATIONAL PERFORMANCE OF CE-MCS VS. CRUDE NSMCS

Case	Metric	Period A	Period B	Period C	Total
CE-MCS	Risk (× 10^{-3})	2.0373	2.2227	3.8679	8.1279
	Time (s)	0.52	3.28	48.03	51.83
Crude NSMC	Risk (× 10^{-3})	2.0467	2.1426	4.1050	8.2943
	Time (s)	5804.26	7872.21	7040.96	20717

C. Composite Power System Risk Indices

The results presented in Sections V-A and V-B clearly establish the superiority of the proposed framework, both, in terms of the proper modeling of wind generation and very high computational performance, over existing methods. In this subsection, we turn our attention to the short-term risk assessment of a wind-integrated composite power system. The contingencies in the transmission system and the line flow limits are now considered. The conditions of RTS are the same as for Table I. The initial wind speed is set to 20 km/h. Table IV summarizes the short-term risk indices for different capacities of the transmission system. A comparison of Table I with Table IV indicates that the short-term risk indices are expectedly higher when the transmission system is included in the assessment. Interestingly, the transmission system's capacities significantly affect the short-term risk indices. With lower transmission capacities, the short-term risk indices are measurably higher. The varying capacities of the transmission system may correspond to the situation of weather-dependent transmission line ratings. Hence, through the proposed framework, power system operators can also recognize the indirect impacts of weather on short-term risk indices. On comparing Table III with Table IV, it can be observed that the computational time increases when the transmission system is considered. This is due to the DC-OPF analysis which is performed for each contingency state for composite systems.

TABLE IV
SHORT-TERM RISK OF COMPOSITE POWER SYSTEM

Capacity	Metric	Period A	Period B	Period C	Total
100 %	Risk (10^{-4})	0.2536	0.9387	2.0397	3.2320
	Time (s)	91.56	378.49	324.75	794.80
90 %	Risk (10^{-3})	0.2832	0.9798	1.1557	2.4187
	Time (s)	70.60	354.36	450.81	875.77
80 %	Risk (10^{-3})	0.4510	1.1156	1.3384	2.9050
	Time (s)	72.66	314.00	246.90	633.56

Fig. 8 is a heat map for the short-term risk at different bus-points when the transmission capacity is 100%. Some buses do not experience any load curtailment and the short-term risk indices at those buses are zero. Also, one can conclude that, from the point of view of short-term risk, bus 18 has the highest risk of load curtailment for these particular hours. Power system operators can utilize such information to provision bus-specific preventive actions. One such action involves re-dispatching the nearby generating units or committing additional units to minimize the risk. Note that these bus-point short-term risk

This article has been accepted for publication in a future issue of this journal, but has not been fully edited. Content may change prior to final publication. Citation information: DOI 10.1109/TPWRS.2018.2881250, IEEE Transactions on Power Systems

9

indices can only be obtained by including the transmission system in the assessment framework.
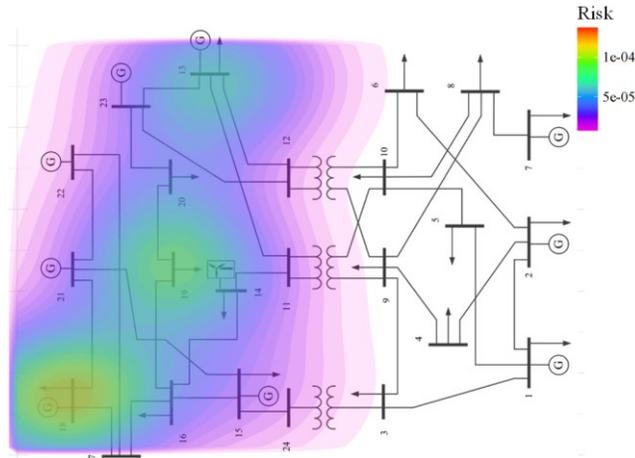
Fig. 8. Heat map for the bus-point short-term risk indices. This figure is generated using [26].

D. Daily Short-Term Risk Indices

This subsection evaluates short-term risk indices for an entire day. The studies are performed for April 2 and the historical mean hourly wind speeds of that day are assumed to be the initial wind speeds. Fig. 8 depicts the total risk for each hour of the day. Interestingly, the total risk is higher during off-peak hours as compared to on-peak hours; this is because few generating stations are committed to supply the load during off-peak hours. Furthermore, most of these committed generating stations comprise only a single unit. Hence, a single generating unit outage might result in load curtailment. On the other hand, many generating stations comprising several generating units are committed during on-peak hours. Wind generation also peaks during these hours. This observation is in stark contrast to the long-term risk assessment, in which the on-peak hours (i.e., the peak load) contribute the most to the long-term risk indices. This highlights the importance of considering the commitment decisions as well as daily variation in load and generation for short-term risk assessment.
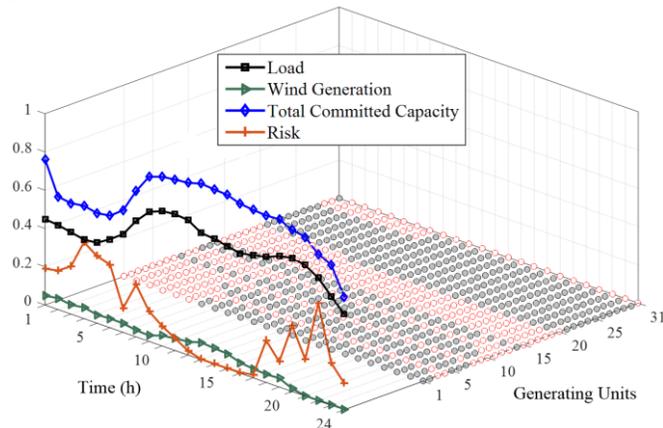
Fig. 9. Daily short-term risk. Load, wind generation and total committed capacity is scaled down by 2000 and shown in MW. Short-term risk is scaled up by 100. Grey dots indicate the committed generating units.

E. Spinning Reserve Assessment

In this subsection, the proposed framework is applied to compare and contrast two deterministic criteria for setting the spinning reserve in power system operation. In criterion 1, the spinning reserve is equal to the capacity of the largest online generating unit, i.e. the N-1 criterion, and in criterion 2, the spinning reserve is set to a certain percentage of load (in this study, 10%) [27]. Fig. 10 illustrates the short-term risk indices and the spinning reserve for the two criteria. As can be seen, for criterion 1, i.e. the N-1, the short-term risk indices are lower compared to criterion 2. However, the total operational costs are the opposite. For criterion 1, the DAUC costs are $ 2.4864 M, whereas for criterion 2, the costs are $ 2.0595 M. This shows that the reliability and costs compete with each other and that higher reliability comes at increased costs. An interesting observation is that, for criterion 1, the spinning reserve remains the same for all hours, however, the short-term risk varies noticeably. This observation demonstrates the shortfall of using inconsistent deterministic criteria for ensuring the reliability during power system operation. On contrary, the power system operators can utilize short-term risk indices to adjust the spinning reserve requirements while ensuring the reliability.
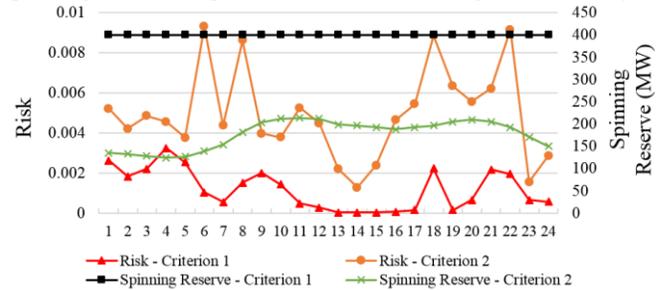
Fig. 10. Short-term risk indices for different spinning reserve criteria.

F. Sensitivity to the Wind Generation Penetration

This subsection examines the effects of the penetration of wind generation on the short-term risk indices. Fig. 11 shows that the total risk monotonically decreases with increasing capacity of the wind farm. For the first and second sub-periods, which are Period A and Period B, the decrease in risk is only marginal. A very slight increase in risk for Period B is observed when the wind farm capacity is 1,250 MW. This is due to the fact that the simulated risk indices are obtained within a certain range of true, actual values (in this case 5%). For the last sub-period, i.e., Period C, a sharp reduction in risk is observed. This observation supports the rationale of utilizing the area risk method to evaluate the partial risks and identify the sub-period(s) that contributes to the short-term risk.
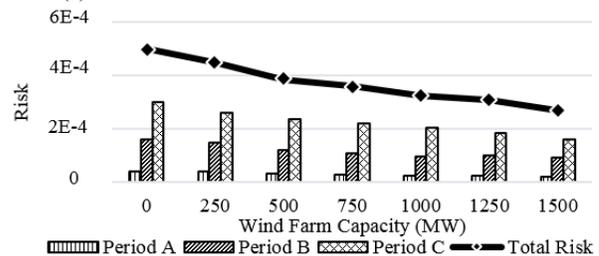
Fig. 11. Short-term risk indices for varying capacities of wind generation. The conditions of RTS are same as that for Table IV (capacity 100%).

G. Sensitivity to the CE Parameters

This subsection examines the effect of parameters of CE optimization on the performance of the proposed framework. The two most important CE parameters are the number of samples for CE optimization N^{CE}, and the multi-level or rarity

parameter ρ [19]. Table V shows the short-term risk indices and corresponding computational times for different values of N^{CE} and ρ, for the case study of Section V.A. As can be observed, the choice of ρ can impact the computational time to a certain degree, however, the short-term risk indices remain the same.

TABLE V
EFFECTS OF N^{CE} AND ρ

N^{CE}	Metric	$\rho = 0.01$	$\rho = 0.03$	$\rho = 0.05$
20,000	Risk (10^{-4})	3.0080	3.0601	3.0402
	Time (s)	21.233	46.80	33.86
30,000	Risk (10^{-4})	3.0274	3.0239	3.0565
	Time (s)	16.37	22.88	14.36
50,000	Risk (10^{-4})	3.0773	3.0911	3.0481
	Time (s)	13.67	32.18	9.88

H. Practical Considerations

As mentioned in the Introduction and shown in Section V.D–V.E, power system operators can utilize the short-term risk indices to evaluate the reliability of the power system in the operational domain. The short-term risk indices calculated using the proposed framework can then be used as input to the conventional power system operation methods. One such scheme for using the short-term risk indices in power system operation has been discussed in [28]. This scheme involves calculating the short-term risk indices after performing the DAUC. Then, the spinning reserve constraints are adjusted for those hours which have higher risk indices and the DAUC is performed again. This ensures that the short-term risk indices remain below a certain pre-defined level for all hours. The proposed framework developed in this framework can easily be appended to such schemes.

VI. CONCLUSION

In this paper, a hybrid framework for the assessment of short-term risk indices of a wind-integrated composite power system is proposed. An analytical technique, i.e., the area risk method, is extended to appropriately consider the impact of wind generation on short-term risk indices through a new reliability modeling approach of wind generation. The modified area risk method is then combined with the CE-MCS, which is an efficient and robust simulation technique, to arrive at a novel framework for the short-term risk assessment of composite power systems.

The case studies performed on the 24-bus IEEE RTS validates the effectiveness of the proposed reliability modeling approach as well as the computational superiority of the proposed framework compared to existing methods. Further, the impacts of the transmission system and daily unit commitment on the short-term risk indices are also explored. Short-term risk indices are significantly affected by the transmission capacities and commitment decisions. Finally, the impact of wind penetration and CE parameters on the short-term risk indices are examined.

REFERENCES

[1] R. Billinton and R. N. Allan, *Reliability Evaluation of Power Systems*, 2nd ed. New York, NY, USA: Plenum, 1996.

[2] W. Li, *Risk Assessment of Power Systems–Models, Methods, and Applications*. New York, NY, USA: IEEE Press, 2005.

[3] L. T. Anstine *et al.*, "Application of probability methods to the determination of spinning reserve requirements for the Pennsylvania-New Jersey-Maryland interconnection," *IEEE Trans. Power App. Syst.*, vol. PAS-82, no. 68, pp. 726–735, Oct. 1963.

[4] S. Thapa, R. Karki, and R. Billinton, "Utilization of the area risk concept for operational reliability evaluation of a wind-integrated power system," *IEEE Trans. Power Syst.*, vol. 28, no. 4, pp. 4771–4779, Nov. 2013.

[5] R. Billinton, B. Karki, R. Karki and G. Ramakrishna, "Unit commitment risk analysis of wind integrated power systems," *IEEE Trans. Power Syst.*, vol. 24, no. 2, pp. 930–939, May 2009.

[6] R. Karki, S. Thapa, and R. Billinton, "A simplified risk-based method for short-term wind power commitment," *IEEE Trans. Sustain. Energy*, vol. 3, no. 3, pp. 498–504, Jul. 2012.

[7] Z. Parvini, A. Abbaspour, M. Fotuhi-Firuzabad, and M. Moeini-Aghtaie, "Operational reliability studies of power systems in presence of energy storage systems," *IEEE Trans. Power Syst.*, vol. 33, no. 4, pp. 3691–3700, Jul. 2018.

[8] S. Thapa, and R. Karki, "Reliability benefit of energy storage in wind integrated power system operation," *IET Gener., Transm., and Distrib.*, vol. 10, no. 3, pp. 807–814, Feb. 2016.

[9] N. Z. Xu, and C. Y. Chung, "Well-being analysis of generating systems considering electric vehicle charging," *IEEE Trans. Power Syst.*, vol. 29, no. 5, pp. 2311–2320, Sep. 2014.

[10] P. Wang, Z. Gao, and L. B. Tjernberg, "Operational adequacy studies of power systems with wind farms and energy storages," *IEEE Trans. Power Syst.*, vol. 27, no. 4, pp. 2377–2384, Nov. 2012.

[11] A. M. Leite da Silva, J. F. Costa Castro, and R. A. González-Fernández, "Spinning reserve assessment under transmission constraints based on cross-entropy method," *IEEE Trans. Power Syst.*, vol. 31, no. 2, pp. 1624–1632, Mar. 2016.

[12] A. M. Leite da Silva, J. F. Costa Castro, and R. Billinton, "Probabilistic assessment of spinning reserve via cross-entropy method considering renewable sources and transmission restrictions," *IEEE Trans. Power Syst.*, vol. 33, no. 4, pp. 4574–4582, Jul. 2018.

[13] Y. Wang *et al.*, "A cross-entropy-based three-stage sequential importance sampling for composite power system short-term reliability evaluation," *IEEE Trans. Power Syst.*, vol. 28, no. 4, pp. 4254–4263, Nov. 2013.

[14] Y. Wang *et al.*, "Adaptive sequential importance sampling technique for short-term composite power system adequacy evaluation," *IET Gener., Transm., and Distrib.*, vol. 8, no. 4, pp. 730–741, Apr. 2014.

[15] T. Ding, C. Li, C. Yan, F. Li, and Z. Bie, "A bilevel optimization model for risk assessment and contingency ranking in transmission system reliability evaluation," *IEEE Trans. Power Syst.*, vol. 32, no. 5, pp. 3803–3813, Sep. 2017.

[16] Y. Feng, W. Wu, B. Zhang, and W. Li, "Power system operation risk assessment using credibility theory," *IEEE Trans. Power Syst.*, vol. 23, no. 3, pp. 1309–1318, Aug. 2008.

[17] B. Hua, Z. Bie, S.K. Au, W. Li, and X. Wang, "Extracting rare failure events in composite system reliability evaluation via subset simulation," *IEEE Trans. Power Syst.*, vol. 30, no. 2, pp. 753–762, Mar. 2015.

[18] R. Y. Rubinstein and D. P. Kroese, *Simulation and the Monte Carlo Methods*, 2nd ed. New York, NY, USA: Wiley, 2007.

[19] R. Y. Rubinstein and D. P. Kroese, *The Cross-Entropy Method*, 1st ed., New York, NY, USA: Springer, 2004.

[20] R. Billinton, R. N. Allan, *Reliability Evaluation of Engineering Systems*, 2nd ed. New York, NY, USA: Springer, 1992.

[21] A. M. Leite da Silva, R. A. González-Fernández, and C. Singh, "Generating capacity reliability evaluation based on Monte Carlo simulation and cross-entropy methods," *IEEE Trans. Power Syst.*, vol. 25, no. 1, pp. 129–137, Feb. 2010.

[22] R. A. González-Fernández, A. M. Leite da Silva, L. C. Resendé, and M. T. Schilling, "Composite systems reliability evaluation based on Monte Carlo simulation and cross-entropy methods," *IEEE Trans. Power Syst.*, vol. 28, no. 4, pp. 4598–4606, Nov. 2013.

[23] E. Tómasson, and L. Söder, "Improved importance sampling for reliability evaluation of composite power systems," *IEEE Trans. Power Syst.*, vol. 32, no. 3, pp. 2426–2434, May 2017.

[24] Reliability Test System Task Force of the IEEE Subcommittee on the Application of Probability Methods, "IEEE reliability test system," *IEEE Trans. Power App. Syst.*, vol. 1, pp. 2047-2054, 1979.

[25] R. Billinton, and W. Wangdee, "Reliability-based transmission reinforcement planning associated with large-scale wind farms," *IEEE Trans. Power Syst.*, vol. 22, no. 1, pp. 34–41, Feb. 2007.

[26] S. Babicki, et al, "Heatmapper: web-enabled heat mapping for all." *Nucleic Acids Res.*, May 2016.

[27] M. A. Ortega-Vazquez, "Optimizing the spinning reserve requirements," Ph.D. thesis, University of Manchester, U.K., 2006.

This article has been accepted for publication in a future issue of this journal, but has not been fully edited. Content may change prior to final publication. Citation information: DOI 10.1109/TPWRS.2018.2881250, IEEE Transactions on Power Systems

11

[28] H. B. Gooi, D. P. Mendes, K. R. W. Bell, and D. S. Kirschen, "Optimal scheduling of spinning reserve," *IEEE Trans. Power Syst.*, vol. 14, no. 4, pp. 1485–1492, Nov. 1999.

Osama Aslam Ansari (S'16) received the B.Eng. degree in electrical engineering from the National University of Sciences and Technology, Islamabad, Pakistan, in 2015, and the M.Sc. degree in electrical engineering from the University of Saskatchewan, Saskatoon, SK, Canada, in 2017, where he is currently pursuing the Ph.D. degree in electrical engineering.

His research interests include power systems reliability, power systems security, and energy storage systems.

C. Y. Chung (M'01–SM'07–F'16) received the B.Eng. (with First Class Honors) and Ph.D. degrees in electrical engineering from The Hong Kong Polytechnic University, Hong Kong, China, in 1995 and 1999, respectively.

He has worked for Powertech Labs, Inc., Surrey, BC, Canada; the University of Alberta, Edmonton, AB, Canada; and The Hong Kong Polytechnic University, China. He is currently a Professor, the NSERC/SaskPower (Senior) Industrial Research Chair in Smart Grid Technologies, and the SaskPower Chair in Power Systems Engineering in the Department of Electrical and Computer Engineering at the University of Saskatchewan, Saskatoon, SK, Canada. His research interests include smart grid technologies, renewable energy, power system stability/control, planning and operation, computational intelligence applications, power markets and electric vehicle charging.

Dr. Chung is an Editor of IEEE Transactions on Power Systems, IEEE Transactions on Sustainable Energy, and IEEE Power Engineering Letters. He is also an IEEE PES Distinguished Lecturer and a Member-at-Large (Global Outreach) of the IEEE PES Governing Board.